Research Project

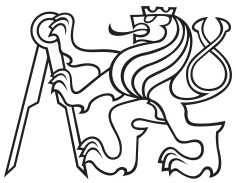

Czech Technical University in Prague

F4

Faculty of Nuclear Sciences and Physical Engineering
Department of Physics

Quantum nanoribbons: geometry, operator theory and spectral analysis

Kateřina Zahradová

Supervisor: Mgr. David Krejčiřík, PhD., DSc.
Field of study: Mathematical Physics
July 2017

Acknowledgements

I would like to thank my supervisor Mgr. David Krejčiřík, Ph.D. DSc. for his patience. Also, I would like to thank my "unofficial consultant" Ing. Tomáš Kalvoda, PhD. without whom the chapters containing numerical mathematics would not be possible.

Declaration

Prohlašuji, že jsem předloženou práci vypracoval samostatně, a že jsem uvedl veškerou použitou literaturu.

V Praze, 10. July 2017

Abstract

This work is dedicated to study of quantum ribbons and their generalisation into higher dimensions. Firstly, facts important for the definition of quantum strips are recalled. Next, one of the possible approach to study of spectra of the Dirichlet Laplacian defined on the strip is presented, especially focusing on the effective dynamics in narrow strips. Lastly, one example of a particular quantum ribbon, the Möbius strip, is presented and its spectrum is treated both analytically and numerically on its various simplified models.

Keywords: quantum ribbons, Möbius strip, spectrum

Supervisor: Mgr. David Krejčiřík, PhD., DSc.

Abstrakt

Tato práce je věnována studiu kvantových stužek a jejich zobecnění do více dimenzí. Nejprve jsou shrnuty poznatky důležité k definici kvantových proužků. Dále je uveden jeden z možných způsobů zkoumání spektra Dirichletovkého Laplaciánu na stužkách, především s důrazem na efektivní dynamiku v tenkých proužcích. Jeden konkrétní příklad, Möbiův proužek, je zde prezentován a jeho spektrum je zkoumáno jak analyticky, tak numericky na jeho různých zjednodušených modelech.

Klíčová slova: kvanotové stužky, Möbiův pásek, spektrum

Překlad názvu: Kvantové nanostužky: geometrie, operátorová teorie a spektrální analýza

Contents

Introduction

The discussion of spectral properties of tubular waveguides in two and three dimensions has started as early as 1989 with a paper by Exner and Šeba [12]. Since then, the question of the influence of geometry on the spectra of a differential operator defined on/in the waveguide has been treated in copious variations, differing in the structure of the cross-section, boundary conditions or the nature of the waveguide.

The area of quantum layers and their properties have been extensively treated in *e.g.* [9] or [5]. For tubular waveguides, the Dirichlet boundary conditions [12, 17, 28], the Neumann boundary conditions [7, 32] or the Robin boundary conditions [11, 15, 34] were considered. The idea of quantum strips has been explored in [26, 27]. A slightly different problem of whole manifolds was treated for instance in [23] or with a more formal approach in [38].

One particular example of a quantum ribbon is the Möbius strip. Over the years, it has been in the center of attention of mathematicians, physicians, and even artists in more than one respect. Its mathematical and physical properties were discussed and dissected in number of papers with numerous settings.

One of the possible criteria of such division is the material of the Möbius strip. The rigid model was examined with respect to magnetization in [16], movement of a free partical [18] or with respect to equilibrium shapes and stress localization in [37]. The Möbius strip made out of graphene was considered in number of papers - *e.g.* for the electronic properties of a topological insulator with respect to the different edges in [19], and the

symmetries and their consequences for chemistry in [14]. Furthermore, the lattice model is also popular – the square lattice Ising model was discussed in [6], persistent currents of non-interacting electron in [39], and the problem of continuous-time quantum walk on the Möbius lattice in [30].

Another viable division is due to the ambient space in which the problem is treated. The former examples as all restricted to three dimensions, however, even generalizations to higher dimensions are being studied in various settings. The problem of spectrum of various differential operators has been studied, *e.g.* [25] for the Klein–Gordon operator in $\mathbb{R}^n$, [24] for the Helmholtz operator on higher dimension Möbius strip embedded in $\mathbb{R}^4$.

This project is divided as follows. The first chapter is devoted to reminder of some basic facts important for institution of quantum strips, followed by their definition. Second chapter addresses the definition of Hamiltonian on the strips and one of the possible treatments for the case of narrow ribbons. Next, some very basic elements of numerical mathematics used later on are presented. In the last chapter, the particular example of the Möbius strip is examined both numerically and analytically.

Chapter 1

Curves

The objective of this chapter is to introduce a notion of (tubular) neighbourhood along a curve. To do this, we recall and restate few important definitions. More detailed information can be found in [22], [29] or [35].

Definition 1.1. A curve in $\mathbb{R}^n$ is a continuously differentiable mapping $c : I \to \mathbb{R}^n$ from any open interval $I := (a, b)$, *i.e.* $a, b \in \mathbb{R} \cup \{-\infty, \infty\}$, into $\mathbb{R}^n$.

Remark. The only restriction on the interval I is its openness – it can be bounded or unbounded.

Definition 1.2. A curve $c : I \to \mathbb{R}^n$ is said to be of class $C^k(I)$ if the derivatives $c', \ldots, c^{(k)}$ exist and are continuous on the interval I. The curve c is of class $C^{k,\alpha}(I)$ if $c \in C^k(I)$ and $c^{(k)}$ satisfies the following condition:

$$(\exists C > 0)\,(\forall x, y \in I)\left(|c^{(k)}(x) - c^{(k)}(y)| \leq C|x - y|^{\alpha}\right).$$

As we are mainly interested in curves of the class $C^{1,1}(I)$, let us rephrase the definition for this particular case: $c \in C^{1,1}(I)$ if c' is continuous and if it satisfies the Lipschitz condition. Furthermore, we will be solely interested in so–called regular curves.

Definition 1.3. A curve is called regular if and only if $c'(t) \neq 0$ for all $t \in I$.

The condition on the first derivative provides the means for defining a tangent (normalized c') along the whole curve c.

Definition 1.4. Let I and J be open intervals in $\mathbb{R}$. Let $c : I \to \mathbb{R}^n$ be a curve and let $h : J \to I$ be a differentiable function. Then the composite

function

$$\tilde{c} := c \circ h : J \to \mathbb{R}^n$$

is a curve and is called the reparametrization of c by h. For $h' \geq 0$ the reparametrization $\tilde{c}$ is called orientation-preserving, resp. orientation-reversing for $h' \leq 0$.

It can be proven that every regular curve c can be reparametrized by its arc–length so that

$$\|c'\| = 1 \quad \forall t \in I.$$

A curve fulfilling the condition above is also called a unit speed curve. From this point onward, we restrict ourselves only to regular unit speed curves.

In order to construct a waveguide along a chosen curve, we need to investigate its moving frame first as it is essential for the desired construction.

Definition 1.5. Let $c : I \to \mathbb{R}^n$ be a curve. A moving n-frame along c is a collection of n differentiable mappings

$$e_i : I \to \mathbb{R}^n, \quad i = 1, \ldots, n,$$

such that for all $t \in I$, $e_i(t) \cdot e_j(t) = \delta_{ij}$, where $\cdot$ denotes the scalar product and δ_{ij} is Kronecker delta. Each $e_i(t)$ is a vector field along c. The parameter t can sometimes be called time as it corresponds to the path taken by the curve and the fields.

We are only concerned about moving frames containing the tangent along the curve and such frames are called adapted. Note that the fact that the frame contains the tangent ensures that the rest of its components is normal to the curve. The reason for this preference is that non-adapted frame generally generates 'singular' ribbons (see Fig.1.1). Let us examine some examples of moving frames before we move further on.

1.1 Moving frames

Moving frames, although very theoretical in construction, are widely used for various practical applications. Their use varies from path planning for robots and CNC ([13]), computer graphics (generation of ribbons, tubes or as mean to define a movement of digital 'cameras', etc. – see [21]) or biology, where the moving frames are used for example as a mean to study the folding of proteins ([31, 33]) or as a way to identify geometrical risk factors for cardiovascular

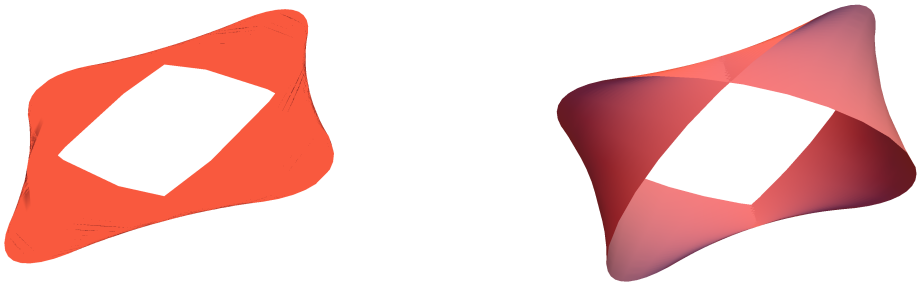

Figure 1.1: Examples of strips constructed with respect to non-adapted rotation-minimizing osculating frame on a circle. Please not that there are points at which the width of the strip is not constant. This is due to the fact that the vector fields used in the construction of this strip are not always normal to the curve.

diseases ([4]). They are also used in study of (quantum) waveguides and ribbons (*e.g.* [28, 20, 10]).

1.1.1 Frenet frame

While discussing moving frames, it is natural to start with the the oldest and most widely know – the Frenet frame.

Consider a regular curve $c : I \to \mathbb{R}^{n+1}$, $c \in C^{n+1}(I)$ such that all $c'(t), c^{(2)}(t), \ldots, c^{(n)}(t)$ are linearly independent for all $t \in I$. Then there exists a unique moving frame $(e_1, \ldots, e_{n+1})$ such that

1. For k, the vectors $1 \leq k \leq n$, $c'(t), \ldots, c^{(k)}(t)$ and $e_1(t), \ldots, e_k(t)$ have the same orientation.
2. $e_1(t), \ldots, e_{n+1}(t)$ have positive orientation.

This frame is called the (distinguished) Frenet frame.

Although the frame is fairly easy to construct using the Gram–Schmidt orthonormalization procedure for the derivatives of the curve, its use in higher

dimensions is impractical due to high demands on the smoothness of the curve. Fortunately, the Frenet frame is not the only frame which can be used to obtain the ribbon.

1.1.2 Relatively parallel adapted frame

The relatively parallel adapted frame, first discussed in three dimensions only in [2], is another possible frame for construction of quantum waveguides and ribbons. Contrary to the Frenet frame, the relatively parallel adapted frame can be constructed for every regular $C^{1,1}$ curve ([40]), meaning for every regular curve $c : I \to \mathbb{R}^{n+1}$, $c \in C^{1,1}(I)$, there exist a collection of vector fields $(T, N_1, \ldots, N_n)$ and functions $k_1, \ldots, k_n : I \to \mathbb{R}$ such that

$$\begin{pmatrix} T \\ N_1 \\ \vdots \\ N_n \end{pmatrix}' = \begin{pmatrix} 0 & k_1 & \ldots & k_n \\ -k_1 & 0 & \ldots & 0 \\ \vdots & \vdots & \ddots & \vdots \\ -k_n & 0 & \ldots & 0 \end{pmatrix} \begin{pmatrix} T \\ N_1 \\ \vdots \\ N_n \end{pmatrix}.$$

The functions $k_1, \ldots, k_n$ are called parallel curvatures. In contrast to the uniqueness of the Frenet frame for a chosen curve, the relatively parallel adapted frame is far from unique and strongly depends on the choice of the initial condition. The construction is as follows. First, choose an arbitrary fixed point on the curve and construct an orthonormal basis at that point such that the first vector in the basis is merged with the tangent. To construct the frame, simply identify the rest of the moving frame as the other components of the basis moved by parallel transport.

1.2 Tubes and Strips

Moving on to the notion of a tube, we define a straight one first.

Definition 1.6. Let $\omega \subset \mathbb{R}^n$ be a bounded open connected set. Then a straight tube Ω_0 is defined as $\Omega_0 := \mathbb{R} \times \omega$. We call ω the cross section.

Remark. From the fact that ω is bounded follows that there exists a real number r, $r < \infty$, such that $r = \sup_{t \in \omega} |t|$, *cf.*. Fig. 1.2.

A straight tube is useful but not very challenging – to obtain a curved one, we need to proceed as follows.

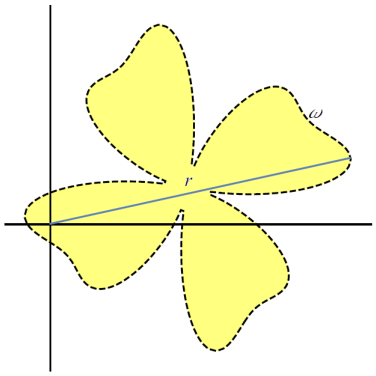

Figure 1.2: An example of a cross-section ω.

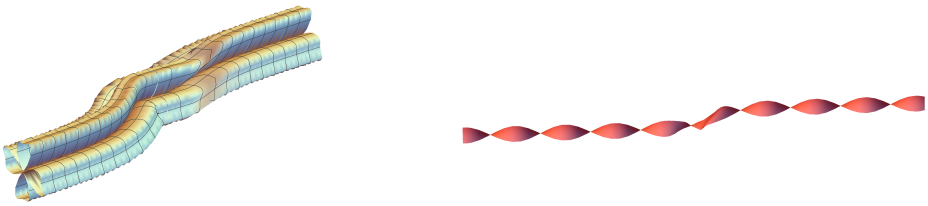

Figure 1.3: An example of a tube and a ribbon constructed along Spivak curve.

Definition 1.7. Be $\Omega_0 = \mathbb{R} \times \omega$ be a straight tube. Let $\Gamma : I \to \mathbb{R}^{n+1}$ be a chosen curve with an adapted moving frame $(T, M_1, \ldots, M_n)$. Let $\mathcal{R}$ be a rotation matrix with entries dependent on $s \in I$. Then we can construct a curved tube along Γ with respect to the rotation $\mathcal{R}$ as

$$\mathcal{L} : \Omega_0 \to \mathbb{R}^{n+1} : (s,t) \mapsto \Gamma(s) + \sum_{i=1}^{n} M_i^{\mathcal{R}}(s) t_i,$$

where $t := (t_1, \ldots, t_n)$ are coordinates on ω and $M_i^{\mathcal{R}}(s) := \mathcal{R}(s) M_i(s)$.

For purposes of this project, we shall constrict ourselves only to tubes such that their cross section is one dimensional, *e.g.* an open interval, and we shall call this special case of tubes as ribbons or strips. An illustration of both a ribbon and a tube can be found on Fig. 1.3. As we are dealing only with strips in the rest of this paper, let us state the definition of a ribbon as used later. Also, even though any adapted frame can be used to construct the strip, we only consider the relatively parallel adapted one for its convenience in higher dimensions.

Definition 1.8. Let $\Gamma : I \to \mathbb{R}^{n+1}$ be a $C^{1,1}$ curve with the relatively parallel adapted frame $(T, N_1, \ldots, N_n)$. Then we define the strip Ω along Γ by the mapping $\mathcal{L} : I \times (-a, a) \to \mathbb{R}^{n+1}$ such that

$$\mathcal{L}(s,t) := \Gamma(s) + t \sum_{i=1}^{n} a_i(s) N_i(s), \tag{1.1}$$

where the functions $a_i : I \to \mathbb{R}$ for all $i \in \{1, \dots, n\}$ satisfy condition $\sum_{i=1}^{n} a_i(s)^2 = 1$ for all $s \in I$.

In order to identify the strip Ω with the Riemannian manifold, we need to impose some further restrictions on the mapping $\mathcal{L}$, namely

1. $\kappa := \sqrt{k_1^2 + \cdots + k_n^2} \in L^\infty(\mathbb{R})$ and $a\|\kappa\|_\infty < 1$;
2. Ω does not overlap itself.

The metric g of the resulting strip is given by $g_{ij} = \partial_i \mathcal{L} \cdot \partial_j \mathcal{L}$. This means that when we calculate the divergence of the gradient, we do not obtain the usual (flat) sum of second derivatives – $\Delta = \sum_i \partial_i^2$. Instead, in local coordinates, the Laplace–Beltrami operator (or just the Laplace operator) can be defined as

$$-\Delta := -|g|^{-1/2} \partial_i |g|^{1/2} g^{ij} \partial_j,$$

where $|g|$ denotes the determinant of the metric g and (g^{ij}) is the inverse to (g_{ij}).

In particular, for a ribbon defined by (1.1), the metric g looks like

$$(g_{ij}) = \begin{pmatrix} h^2 & 0 \\ 0 & 1 \end{pmatrix}, \tag{1.2}$$

where

$$h^2 = (1 - t a_i k_i)^2 + t^2 \sum_{i=1}^{n} \dot{a}_i^2 \tag{1.3}$$

and k_i are parallel curvatures of the relatively parallel adapted frame used in the definition of the strip. Additionally, the resulting Laplace–Beltrami operator for such ribbon is given by

$$-\Delta = -\frac{1}{h}\,\partial_s \,\frac{1}{h}\,\partial_s - \frac{1}{h}\,\partial_t\, h\, \partial_t. \tag{1.4}$$

Chapter 2

Quantum ribbons

In this chapter, the effective potential for quantum ribbons in higher dimensions is derived and compared with the one already known for the three dimensional case.

After we defined the curved ribbon it the previous chapter, let us examine notion of a free particle constricted to the strip, closely following the process of [9]. To simulate a free particle confined in an infinite potential well Ω, we consider a free Laplacian with Dirichlet boundary conditions simulating this infinite drop of potential on the boundary of the strip. Setting the respective physical constants to suitable values, we can establish the Hamiltonian $\tilde{H}$ as the Dirichlet Laplacian

$$\tilde{H} := -\Delta_D^\Omega \quad \text{on} \quad L^2(\Omega),$$

defined on an open set $\Omega \subset \mathbb{R}^{n+1}$ as the Friedrich extension of the operator $-\Delta$ with domain $C_0^\infty(\Omega)$ – see *e.g.* [36] for more details.

In order to obtain an alternative and more suitable form of the Hamiltonian for our study, one performs a unitary transformation as follows:

$$U : L^2(\Omega) \to L^2(\Omega_0) : \{\psi \mapsto U\psi := g^{\frac{1}{4}}\psi \circ \phi\}.$$

This leaves us with the unitary equivalent operator

$$H := U\tilde{H}U^{-1} = -g^{-\frac{1}{4}}\partial_i g^{\frac{1}{2}} g^{ij}\partial_j g^{-\frac{1}{4}} \tag{2.1}$$

The domain of this operator is

$$\mathsf{D}(H) := \{\psi \in W^{2,2}(\Omega_0) | \forall s \in I \,:\, \psi(s,-a) = \psi(s,a) = 0\}.$$

The expression (2.1) can be further rearranged by commuting $g^{-\frac{1}{4}}$ with the partial derivatives into

$$H = -\partial_i g^{ij} \partial_j + V,$$

where

$$V = F_{,i} g^{ij} F_{,j} + (F_{,i} g^{ij})_{,j}\,, \quad F = \log g^{\frac{1}{4}}.$$

When we use the expression (1.2) and compute the potential, we obtain the following expression for V in terms of the function h

$$V = -\frac{5}{4}\frac{h_{,s}^2}{h^4} + \frac{1}{2}\frac{h_{,ss}}{h^3} - \frac{1}{4}\frac{h_{,t}^2}{h^2} + \frac{1}{2}\frac{h_{,tt}}{h}.$$

Now, as the present day interest particularly resides in nano–materials and their properties, we will further examine the case when the width of the ribbon tends to zero, *i.e.* we consider the limit $a \to 0$.

Due to the form of h (see (1.3)) and its derivatives, the terms containing differentiation with respect to s tend to zero as a tends to zero. The acquired effective potential then has the following form

$$V_{\text{eff}} = -\frac{1}{4a^2}\frac{h_{,t}^2}{h^2} + \frac{1}{2a^2}\frac{h_{,tt}}{h}\bigg|_{a=0}.$$

Using the explicit expression (1.3) with the limit $a \to 0$ meaning $h \to 1$, we obtain the final formula

$$V_{\text{eff}} = -\frac{1}{4}\left(\sum_{i=1}^{n} k_i a_i\right)^2 + \frac{1}{2}\left(\sum_{i=1}^{n} \dot{a}_i\right)^2.$$

It can be further reduced if we introduce the following simplifying notation $\vec{a}\cdot\vec{k} := \sum_{i=1}^{n} k_i a_i$ and $|\dot{\vec{a}}| := \sum_{i=1}^{n} \dot{a}_i$ to

$$V_{\text{eff}} = -\frac{1}{4}\left(\vec{a}\cdot\vec{k}\right)^2 + \frac{1}{2}|\dot{\vec{a}}|^2. \tag{2.2}$$

Moving on to the three dimensional case, one finds out that the situation is much simpler there. Let us recall the formula (1.1) for the curved strip in any dimension:

$$\mathcal{L}(s,t) := \Gamma(s) + t\sum_{i=1}^{n} a_i(s) N_i(s).$$

Following the idea that the functions a_i serve here as the first row of a rotation matrix, the expression for an arbitrary ribbon in three dimensions can be expressed as

$$\mathcal{L}(s,t) := \Gamma(s) + t\left[N_1(s)\cos\left(\theta(s)\right) - N_2(s)\sin\left(\theta(s)\right)\right],$$

where N_1, N_2 are normals from the relatively parallel adapted frame and $\theta : I \to \mathbb{R}$ is some bounded C^1 function facilitating twisting of the ribbon.

Following the same process as outlined above, we arrive at the following formula for the effective potential

$$V_{\text{eff}} = -\frac{1}{4}\left[k_1^2\cos^2\theta + k_1k_2\sin 2\theta + k_2^2\sin^2\theta\right] + \frac{1}{2}\dot{\theta}^2. \tag{2.3}$$

The obvious similarity is the repulsive interaction introduced by the differential of the twisting term in both expressions (2.2) and (2.3) and the attractive interaction established by both the curvatures and the twisting. The nature of these terms in three dimensions have been proven in [26, 27] and we, for the time being without a proof, expect that the effect of these terms on the spectrum of the Hamiltonian in higher dimensions is the same.

Chapter 3

Numerical analysis

In this chapter, some basic elements of numerical mathematics used in the study of the spectrum of the Laplace–Beltrami operator are presented. For the numerical analysis in Chapter 4, we used the Finite Difference Method (FDM). As this paper is not primarily concerned in the topic of programming and numerical solutions, we provide only a review of the necessary facts.

One of many ways how to approximate the solution of partial differential equations is to use the finite difference method. This approach is based on substituting the derivatives with finite differences. In other words, we discretise the problem and solve it as a system of linear algebraic equations.

Let us constrict ourselves to a one–dimensional example for the moment. Be $f : (a, b) \to \mathbb{R}$ a differentiable function. Then in the FDM, the first derivative of f can be substituted using different finite differences:

$$\begin{aligned}
&\text{forward difference:} && f'(x) \approx \frac{f(x+h) - f(x)}{h}, \\
&\text{symetric difference:} && f'(x) \approx \frac{f(x+h) - f(x-h)}{2h}, \\
&\text{backward difference:} && f'(x) \approx \frac{f(x) - f(x-h)}{h}.
\end{aligned}$$

Each differences can be useful in different conditions. The second derivative, f'', is usually replaced by the following expression

$$f''(x) \approx \frac{f(x+h) - 2f(x) + f(x-h)}{h^2},$$

which can be obtained by combining the forward and backward difference for the first derivative and then using the symmetric one. When applied

to higher–dimensional problems, the differences are done in each variable separately, *i.e.* (using the forward difference)

$$\psi_{,s}(s,t) \approx \frac{\psi(s+h,t) - \psi(s,t)}{h}.$$

We base the discretization on a simple rectangular grid (see Fig. 3.1). Effectively we approximate the operator in question by a matrix operator acting in vector space $\mathbb{C}^N$ (with possibly large N).

The finer the grid (*i.e.* the larger the matrix) is, the better approximation of the original spectrum we expect to get as the differences are closer to the values of the actual derivatives. This effect is demonstrated later on in Section 4.3.

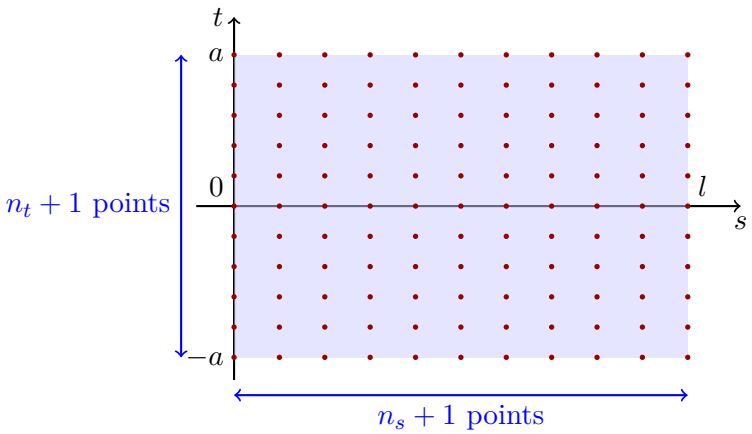

Figure 3.1: Rectangular grid formed by $(n_t + 1) \cdot (n_s + 1)$ points from the strip $(0, l) \times (-a, a)$.

Chapter 4

Möbius strip

One example of a closed ribbon in $\mathbb{R}^3$ is the Möbius strip. Our choice of this particular manifold for our study is caused by its unorientability and its similarity to either a cylinder or an annulus (Fig. 4.1). For the purpose of this paper, we consider a circular Möbius strip with constant twisting defined as follows.

Let the base circle be prescribed as

$$\varphi : (0, 2\pi) \to \mathbb{R}^3 : s \mapsto \left(R\cos\frac{s}{R}, R\sin\frac{s}{R}, 0 \right),$$

for some $R > 0$. In this case, there is no advantage of choosing the relatively parallel adapted frame over the Frenet frame, as the latter is correctly defined for this choice of curve and in fact coincides with the relatively parallel one, if the initial triad is chosen as the vectors of the Frenet frame. By easy calculations, we arrive to the following frame components:

$$\begin{aligned} T(s) &= \left(-\sin\frac{s}{R}, \cos\frac{s}{R}, 0 \right), \\ N(s) &= \left(-\cos\frac{s}{R}, -\sin\frac{s}{R}, 0 \right), \\ B(s) &= (0, 0, 1), \\ \kappa(s) &= \frac{1}{R}, \end{aligned}$$

as the tangent, the principal normal, the binormal and the curvature respec-

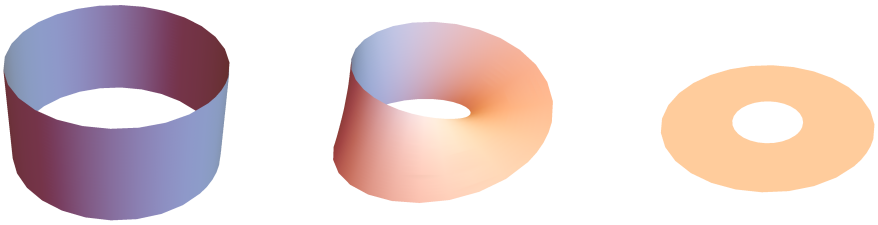

Figure 4.1: By different choice of the function θ in construction of the ribbon (1.1), we can get different results. This particular example illustrates a ribbon along a circle with the $\theta = \frac{\pi}{2}, \frac{s}{2R}$ or 0 for the cylinder, Möbius strip and annulus respectively.

tively. The time development of the frame then is given by

$$\begin{pmatrix} T \\ N \\ B \end{pmatrix}^{\cdot} = \begin{pmatrix} 0 & \kappa & 0 \\ -\kappa & 0 & 0 \\ 0 & 0 & 0 \end{pmatrix} \begin{pmatrix} T \\ N \\ B \end{pmatrix}.$$

We construct the Möbius strip by (1.1) with a special choice on the "twisting" function θ. As we aim to obtain only a half of a twist for one rotation, the easiest way to do that is to set $\theta := \frac{s}{2R}$. The strip is then given by the following mapping

$$\mathcal{L}(s,t) := \varphi(s) + t\left[N(s)\cos\frac{s}{2R} - B(s)\sin\frac{s}{2R}\right],$$

for $s \in (0, 2\pi)$ and $t \in (-a, a)$. This mapping induces by $g_{ij} := \partial_i\mathcal{L} \cdot \partial_j\mathcal{L}$ the metric

$$(g_{ij}) = \begin{pmatrix} h^2 & 0 \\ 0 & 1 \end{pmatrix},$$

where

$$h(s,t) = \sqrt{\left(1 - \frac{t}{R}\cos\frac{s}{2R}\right)^2 + \left(\frac{t}{2R}\right)^2}.$$

When computed, the Laplace–Beltrami operator (1.4) is not separable in this case. Therefore, some solvable approximations of the full Möbius strip as well as numerical solutions of these approximations are presented instead.

4.1 Fake Möbius strip

We will start the discussion of approximative models with the simplest setting – the fake (or flat) Möbius strip. In this model, the Möbius strip is perceived as a flat rectangle of the desired size with two of the opposing sides

Figure 4.2: The fake Möbius strip - a rectangle with two of the opposite sides identified by the arrows.

identified as indicated at Fig. 4.2. The sacrifice of the bending means that the Laplace–Beltrami operator is separable and thus the problem be solved analytically as indicated below.

We consider the following boundary value problem:

$$\begin{cases} -\Delta\psi = \lambda\psi\,, & \text{in} \quad (0,l)\times(-a,a)\,, \\ \psi(s,\pm a) = 0\,, & \forall s\in(0,l)\,, \\ \psi(0,t) = \psi(l,-t)\,, & \forall t\in(-a,a)\,, \\ \partial_1\psi(0,t) = \partial_1\psi(l,-t)\,, & \forall t\in(-a,a)\,. \end{cases} \tag{4.1}$$

This is also the eigenvalue problem $H\psi = \lambda\psi$ for the self–adjoint operator H in $L^2\left((0,l)\times(-a,a)\right)$ defined as

$$\begin{aligned} H\psi &:= -\Delta\psi \\ \mathsf{D}(H) &:= \Big\{\psi\in W^{2,2}\left((0,l)\times(-a,a)\right)\Big|\ \psi \text{ satisfies the boundary} \\ &\qquad\qquad \text{conditions of (4.1)}\Big\}. \end{aligned}$$

The spectrum of the operator H can be found by considering the (extended) periodic problem

$$\begin{cases} -\Delta\phi = \mu\phi\,, & \text{in} \quad (-l,l)\times(-a,a)\,, \\ \phi(s,\pm a) = 0\,, & \forall s\in(-l,l)\,, \\ \phi(-l,t) = \phi(l,t)\,, & \forall t\in(-a,a)\,, \\ \partial_1\phi(-l,t) = \partial_1\phi(l,t)\,, & \forall t\in(-a,a)\,. \end{cases} \tag{4.2}$$

More precisely, (4.2) is the eigenvalue problem $T\phi = \mu\phi$ for the self–adjoint operator T in an extended Hilbert space $L^2\left((-l,l)\times(-a,a)\right)$ defined as

$$\begin{aligned} T\phi &:= -\Delta\phi\,, \\ \mathsf{D}(T) &:= \Big\{\phi\in W^{2,2}((-l,l)\times(-a,a))\Big|\ \phi \text{ satisfies the boundary} \\ &\qquad\qquad \text{conditions of (4.2)}\Big\}. \end{aligned}$$

This problem can be solved by separation of variables and the spectrum of T is well known in the form

$$\sigma(T) = \left\{\left(\frac{m\pi}{l}\right)^2 + \left(\frac{n\pi}{2a}\right)^2\right\}_{m\in\mathbb{Z},n\in\mathbb{N}},$$

where the convention $\mathbb{N} = \{1, 2, \dots\}$ is used. The corresponding eigenfunctions of T are

$$\phi_{m,n} = \varphi_m(s)\chi_n(t),$$

where

$$\varphi_m(s) := \sqrt{\frac{1}{2l}}\, e^{i\frac{\pi}{l}ms}\,, \qquad \chi_n(t) := \begin{cases} \sqrt{\frac{1}{a}}\,\cos(\frac{n\pi}{2a}t) & \text{if } n \text{ is odd}\,, \\ \sqrt{\frac{1}{a}}\,\sin(\frac{n\pi}{2a}t) & \text{if } n \text{ is even}\,. \end{cases}$$

The eigenfunctions $\{\phi_{m,n}\}_{m\in\mathbb{Z},n\in\mathbb{N}}$ of the self–adjoint operator T also form a complete orthonormal set in $L^2\left((-l,l)\times(-a,a)\right)$ (see [3]). By symmetry properties of φ_m and χ_n, we have

$$\begin{aligned} \phi_{m,n}(l,-t) &= (-1)^{m+n+1}\,\phi_{m,n}(0,t)\,, \\ \partial_1\phi_{m,n}(l,-t) &= (-1)^{m+n+1}\,\partial_1\phi_{m,n}(0,t)\,. \end{aligned}$$

Therefore we see that $\phi_{m,n}$ satisfies the boundary conditions of (4.1) if, and only if, $m+n$ is odd. Consequently,

$$\sigma(H) \supset \left\{ \left(\frac{m\pi}{l}\right)^2 + \left(\frac{n\pi}{2a}\right)^2 \right\}_{m\in\mathbb{Z},\ n\in\mathbb{N},\ m+n \text{ is odd}} \tag{4.3}$$

and the corresponding normalised eigenfunctions of H are given by the restrictions

$$\psi_{m,n} := \sqrt{2}\,\phi_{m,n} \restriction (0,l)\times(-a,a)\,, \qquad m\in\mathbb{Z},\ n\in\mathbb{N},\ m+n \text{ is odd}\,.$$

To show that the right-hand side of (4.3) determines *all* the eigenvalues of H, we need the following result.

Proposition 1. $\{\psi_{m,n}\}_{m\in\mathbb{Z},\ n\in\mathbb{N},\ m+n \text{ is odd}}$ is a complete orthonormal set in $L^2((0,l)\times(-a,a))$.

Proof. The property that $\{\phi_{m,n}\}_{m\in\mathbb{Z},\ n\in\mathbb{N}}$ is a complete orthonormal set in $L^2((-l,l)\times(-a,a))$ is equivalent to the validity of the Parseval equality

$$\|f\|^2 = \sum_{m\in\mathbb{Z},\,n\in\mathbb{N}} |(\phi_{m,n}, f)|^2 \tag{4.4}$$

for every $f\in L^2((-l,l)\times(-a,a))$. Given an arbitrary $g\in L^2((0,l)\times(-a,a))$, we define the extension

$$f(s,t) := \begin{cases} g(s,t) & \text{if} \quad s>0\,, \\ g(s+l,-t) & \text{if} \quad s<0\,. \end{cases}$$

By an obvious integral substitution, it is straightforward to check the identity

$$\|f\|^2 = 2\,\|g\|^2\,. \tag{4.5}$$

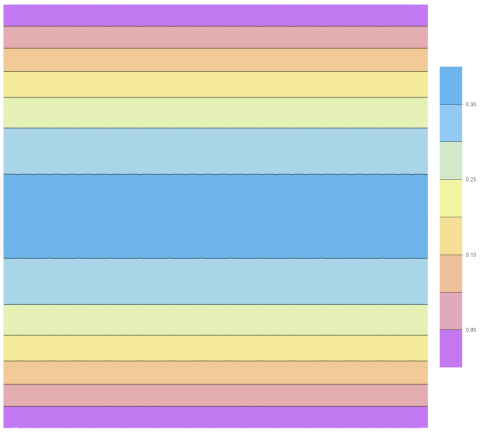

Figure 4.3: Contour plot of $\psi_{0,1}$, the eigenfunction corresponding to the lowest eigenvalue of the fake Möbius strip.

At the same time, using in addition to the substitution the symmetry properties of φ_m and χ_n, we have

$$(\phi_{m,n}, f) = \frac{1}{\sqrt{2}} \left[1 + (-1)^{m+n+1}\right] (\psi_{m,n}, g)\,. \tag{4.6}$$

Putting (4.5) and (4.6) into (4.4), we get the Parseval inequality

$$\|g\|^2 = \sum_{\substack{m\in\mathbb{Z},\, n\in\mathbb{N} \\ m+n \text{ is odd}}} |(\psi_{m,n}, g)|^2\,,$$

which is equivalent to the desired completeness result. □

As a consequence of this proposition, we conclude with the desired result

$$\sigma(H) = \left\{ \left(\frac{m\pi}{l}\right)^2 + \left(\frac{n\pi}{2a}\right)^2 \right\}_{m\in\mathbb{Z},\ n\in\mathbb{N},\ m+n \text{ is odd}}.$$

Remark 4.1. The lowest eigenvalue

$$\lambda_{0,1} = \left(\frac{\pi}{2a}\right)^2$$

is simple and the corresponding eigenfunction $\psi_{0,1}$ (see Fig. 4.3) is positive. The eigenvalues $\lambda_{m,n}$ with $m \neq 0$ are always degenerate. In particular, this is true for the second eigenvalue

$$\min\{\lambda_{1,2} = \lambda_{-1,2}, \lambda_{2,1} = \lambda_{-2,1}\}.$$

Furthermore, if $l = 2a$ then the second eigenvalue $\frac{5\pi^2}{4a^2}$ has multiplicity *four*! We suspect that in this case there will be an eigenfunction with a closed nodal line, which is an interesting phenomenon.

We call (4.1) the eigenvalue problem for the fake Möbius strip, because the correct operator unitarily equivalent to the Laplace–Beltrami operator on the Möbius strip with Dirichlet boundary conditions is not H but (at least in the limit when a tends to zero)

$$H + V_0 \qquad \text{with} \qquad V_0(s,t) := -\frac{\pi^2}{2l^2}\,\cos(2\tfrac{\pi}{l}s)\,. \tag{4.7}$$

Unfortunately, the extension procedure above does not seem to extend to $H + V_0$. At this moment, by a simple test-function argument, we just have the result

$$\min\sigma(H+V_0) \leq \lambda_{0,1}\,. \tag{4.8}$$

By improving the test function, one can even show that the inequality is strict and get a quantitative estimate on the deficit.

Proposition 2. We have

$$\min\sigma(H+V_0) \leq \lambda_{0,1} - \frac{14\sqrt{3}-24}{l^2}\,.$$

Proof. Inequality (4.8) is obtained by using the test function $\psi := \psi_{0,1}$ in the variational characterisation of the lowest eigenvalue of $H + V_0$:

$$\min\sigma(H+V_0) = \inf_{\substack{\psi\in\mathsf{D}(h)\\ \psi\neq 0}} \frac{\displaystyle\int_0^l\int_{-a}^a |\nabla\psi(s,t)|^2\,\mathrm{d}t\,\mathrm{d}s + \int_0^l\int_{-a}^a V_0(s,t)\,|\psi(s,t)|^2\,\mathrm{d}t\,\mathrm{d}s}{\displaystyle\int_0^l\int_{-a}^a |\psi(s,t)|^2\,\mathrm{d}t\,\mathrm{d}s}\,. \tag{4.9}$$

Here h denotes the form associated with H. One has

$$\mathsf{D}(h) = \left\{ \phi\in W^{1,2}((-l,l)\times(-a,a)) \,\middle|\, \begin{array}{ll} \forall s\in(0,l)\,, & \psi(s,\pm a)=0 \\ \forall t\in(-a,a)\,, & \psi(0,t)=\psi(l,-t) \end{array} \right\},$$

where the boundary values are understood in the sense of traces. The result (4.8) follows at once by noticing that $\psi_{0,1}$ is independent of s, V_0 is independent of t and $\int_0^l V_0(s,t)\,\mathrm{d}s = 0$.

Now we take a more refined test function

$$\psi(s,t) := \varphi(s)\,\chi_1(t) \qquad \text{with} \qquad \varphi(s) := \begin{cases} l - p\,s & \text{if} \quad s \leq l/2\,, \\ l - p\,(l-s) & \text{if} \quad s > l/2\,, \end{cases}$$

where p is a real parameter. Notice that φ is Lipschitz continuous, symmetric with respect to the middle point $l/2$ and chosen in such a way that for positive p it "localises" on the negative part of the potential V_0. Restricting the infimum in (4.9) to this class of test functions, an explicit computation of the integrals yields

$$\min\sigma(H+V_0) - \lambda_{0,1} = \frac{1}{l^2}\inf_{p\in\mathbb{R}} \frac{3p\,(5p-4)}{p\,(p-6)+12}\,.$$

The infimum on the right-hand side is achieved for

$$p := \frac{2}{13}\left(15 - 7\sqrt{3}\right)$$

and this value gives the desired upper bound of the proposition. □

Remark 4.2. We have

$$14\sqrt{3} - 24 \approx 0.2487.$$

It should be possible to further improve the result, by extending the class of considered test functions.

4.2 The not-so-fake Möbius strip

In this section, more realistic model of the Möbius strip is discussed. It arises from the fake strip, but we add the effective potential V_0 as defined in (4.7), also see Chapter 2. Even though the model is still flat, the addition of V_0 makes it applicable to very narrow strips (when their width tends to zero).

Consider the boundary value problem

$$\begin{cases} (-\Delta + V_0(s,t))\psi = \lambda\psi\,, & \text{in} \quad (0,l)\times(-a,a)\,,\\ \psi(s,\pm a) = 0\,, & \forall s \in (0,l)\,,\\ \psi(0,t) = \psi(l,-t)\,, & \forall t \in (-a,a)\,,\\ \partial_1\psi(0,t) = \partial_1\psi(l,-t)\,, & \forall t \in (-a,a)\,, \end{cases} \tag{4.10}$$

where l and a are arbitrary positive numbers and the potential V_0 is defined in (4.7). More precisely, (4.10) is the eigenvalue problem $K\psi = \lambda\psi$ for the self-adjoint operator K in $L^2((0,l)\times(-a,a))$ defined as follows:

$$K\psi := (-\Delta + V_0(s,t))\psi\,,$$
$$\mathsf{D}(K) := \Big\{\psi \in W^{2,2}((0,l)\times(-a,a)) \Big| \psi \text{ satisfies the boundary conditions of (4.10)}\Big\}.$$

The spectrum of K can be found by again considering the periodic problem

$$\begin{cases} (-\Delta + V_0(s,t))\phi = \zeta\phi\,, & \text{in} \quad (-l,l)\times(-a,a)\,,\\ \phi(s,\pm a) = 0\,, & \forall s \in (-l,l)\,,\\ \phi(-l,t) = \phi(l,t)\,, & \forall t \in (-a,a)\,,\\ \partial_1\phi(-l,t) = \partial_1\phi(l,t)\,, & \forall t \in (-a,a)\,. \end{cases} \tag{4.11}$$

More precisely, (4.11) is the eigenvalue problem $S\phi = \zeta\phi$ for the self-adjoint operator S in an extended Hilbert space $L^2((-l,l)\times(-a,a))$ defined as follows:

$$\begin{aligned} S\phi &:= (-\Delta + V_0(s,t))\phi\,, \\ \mathsf{D}(S) &:= \Big\{\phi \in W^{2,2}((-l,l)\times(-a,a)) \Big| \phi \text{ satisfies the boundary conditions of (4.11)}\Big\}. \end{aligned}$$

The eigenvalues and eigenfunctions of S can be found by separation of variables. In the variable t we get the same result as in the previous section. The normalised eigenfunctions of $-\frac{\mathrm{d}^2}{\mathrm{d}t^2}$ in $L^2((-a,a),\,\mathrm{d}t)$ with Dirichlet boundary conditions are numbered by $n \in \mathbb{N}$ and given by

$$\chi_n(t) := \begin{cases} \sqrt{\frac{1}{a}}\,\cos(\frac{n\pi}{2a}t) & \text{if } n \text{ is odd}\,, \\ \sqrt{\frac{1}{a}}\,\sin(\frac{n\pi}{2a}t) & \text{if } n \text{ is even}\,. \end{cases}$$

The corresponding eigenvalues are

$$\left(\frac{n\pi}{2a}\right)^2, \quad n \in \mathbb{N}. \tag{4.12}$$

The case of the second variable s is a little bit more involved. After the separation we arrive at the following differential equation

$$-\varphi''(s) - \frac{\pi^2}{2l^2}\cos\left(\frac{2\pi}{l}s\right)\varphi(s) = \nu\varphi(s)\,. \tag{4.13}$$

It turns out that this is the Mathieu differential equation. Before we proceed any further let us first review basic properties of Mathieu functions.

Remark 4.3 (Mathieu functions). We use the following notation (see also [8, §28.2]). Fix $q, \mu \in \mathbb{R}$ and consider the ordinary differential equation

$$y''(\eta) + (\mu - 2q\cos(2\eta))y(\eta) = 0\,. \tag{4.14}$$

This equation has a 2π-periodic solution if and only if $\mu = a_r(q)$ or $\mu = b_r(q)$, where $a_r(q)$, $r \in \mathbb{N}_0$, and $b_r(q)$, $r \in \mathbb{N}$, are the so called Mathieu characteristic values. These characteristic values satisfy

$$\begin{aligned} &q > 0: \ a_0 < b_1 < a_1 < b_2 < a_2 < \cdots\,, \\ &q < 0: \ a_0 < a_1 < b_1 < b_2 < a_2 < \cdots\,, \\ &q = 0: \ a_r(0) = b_r(0) = r^2\,. \end{aligned} \tag{4.15}$$

The Mathieu integral order functions $\mathrm{ce}_r(\eta,q)$, $r \in \mathbb{N}_0$, and $\mathrm{se}_r(\eta,q)$, $r \in \mathbb{N}$, are defined in the following way: $\mathrm{ce}_r(\eta,q)$ is the even solution of (4.14) with $\mu = a_r(q)$ and $\mathrm{se}_r(\eta,q)$ is the odd solution of (4.14) with $\mu = b_r(q)$. Both $\mathrm{ce}_r(\cdot,q)$ and $\mathrm{se}_r(\cdot,q)$ are 2π-periodic. Moreover, $\mathrm{ce}_{2r}(\cdot,q)$ and $\mathrm{se}_{2r+2}(\cdot,q)$ are π-periodic and $\mathrm{ce}_{2r+1}(\cdot,q)$ and $\mathrm{se}_{2r+1}(\cdot,q)$ are antiperiodic with antiperiod

π. For any $q \in \mathbb{R}$, the integral order Mathieu functions $\mathrm{ce}_r(\eta, q)$ and $\mathrm{se}_r(\eta, q)$ taken together form an orthogonal basis in $L^2\big((-\pi, \pi),\, \mathrm{d}\eta\big)$ (see [1, §20.5]).

We assume both $\mathrm{ce}_r(\eta, q)$ and $\mathrm{se}_r(\eta, q)$ are normalised to $\sqrt{\pi}$ in $L^2\big(-\pi, \pi),\, \mathrm{d}\eta\big)$, *i.e.* the equalities

$$\int_{-\pi}^{\pi} \big|\,\mathrm{ce}_r(\eta, q)\big|^2\,\mathrm{d}\eta = \int_{-\pi}^{\pi} \big|\,\mathrm{se}_r(\eta, q)\big|^2\,\mathrm{d}\eta = \pi$$

hold for all possible values of r. This convention is in agreement with [8] and it is respected by *Mathematica*, too. The (anti)periodicity then implies

$$\int_{0}^{\pi} \big|\,\mathrm{ce}_r(\eta, q)\big|^2\,\mathrm{d}\eta = \int_{0}^{\pi} \big|\,\mathrm{se}_r(\eta, q)\big|^2\,\mathrm{d}\eta = \frac{\pi}{2}\,.$$

Let us return to the equation (4.13). Employing a simple change of the independent variable, $\eta = \frac{\pi}{l}s$, we immediately get the Mathieu equation (4.14) (with $q = -\frac{1}{4}$ and $\mu = \frac{l^2}{\pi^2}\nu$). Thus the equation (4.13) has the following $2l$-periodic and normalised solutions if and only if ν satisfies one of the indicated conditions

$$\varphi_r^{(1)}(s) := \frac{1}{\sqrt{\pi}}\,\mathrm{se}_r\left(\frac{\pi}{l}s, -\frac{1}{4}\right), \qquad \text{if } b_r\left(-\frac{1}{4}\right) = \frac{l^2}{\pi^2}\nu\,,\ \text{for some } r \in \mathbb{N}\,, \tag{4.16}$$

$$\varphi_r^{(2)}(s) := \frac{1}{\sqrt{\pi}}\,\mathrm{ce}_r\left(\frac{\pi}{l}s, -\frac{1}{4}\right), \qquad \text{if } a_r\left(-\frac{1}{4}\right) = \frac{l^2}{\pi^2}\nu\,,\ \text{for some } r \in \mathbb{N}_0\,. \tag{4.17}$$

The eigenvalues of S therefore are

$$\sigma(S) = \left\{\left(\frac{n\pi}{2a}\right)^2 + \frac{\pi^2}{l^2}a_r\left(-\frac{1}{4}\right)\right\}_{\substack{n\in\mathbb{N}\\ r\in\mathbb{N}_0}} \cup \left\{\left(\frac{n\pi}{2a}\right)^2 + \frac{\pi^2}{l^2}b_r\left(-\frac{1}{4}\right)\right\}_{\substack{n\in\mathbb{N}\\ r\in\mathbb{N}}}.$$

The corresponding normalised eigenfunctions form an orthogonal basis of $L^2\big((-l, l)\times(-a, a),\, \mathrm{d}s\mathrm{d}t\big)$,

$$\begin{aligned}\phi_{r,n}^{(1)}(s,t) &:= \varphi_r^{(1)}(s)\,\chi_n(t), \quad r \in \mathbb{N}\,,\ n \in \mathbb{N}\,,\\ \phi_{r,n}^{(2)}(s,t) &:= \varphi_r^{(2)}(s)\,\chi_n(t), \quad r \in \mathbb{N}\,,\ n \in \mathbb{N}\,.\end{aligned}$$

Let us now find the eigenfunctions and eigenvalues of the not-so-fake Möbious strip operator K. Note that for any $j = 1, 2$ the functions $\varphi_r^{(j)}$ are antiperiodic, resp. periodic, with antiperiod l, resp. period l, whenever r is odd, resp. even. Using this observation we establish the following key property of the eigenfunctions of S, namely

$$\begin{aligned}\phi_{r,n}^{(j)}(s+l, -t) &= \varphi_r^{(j)}(s+l)\cdot\chi_n(-t) = (-1)^r\varphi_r^{(j)}(s)\cdot(-1)^{n+1}\chi_n(t)\\ &= (-1)^{r+n+1}\phi_{r,n}^{(j)}(s,t)\,,\end{aligned} \tag{4.18}$$

for any $j = 1, 2$ and all permissible r and n. In particular, setting $s = 0$ in the last equation we have

$$\phi^{(j)}_{r,n}(l, -t) = (-1)^{r+n+1}\phi^{(j)}_{r,n}(0, t)\,.$$

and so $\phi^{(j)}_{r,n}$, $j = 1, 2$, satisfies the boundary conditions of (4.10) if and only if $r + n$ is *odd*. Consequently,

$$\sigma(K) \supset \left\{\left(\frac{n\pi}{2a}\right)^2 + \frac{\pi^2}{l^2}a_r\left(-\frac{1}{4}\right)\right\}_{\substack{n\in\mathbb{N}\\ r\in\mathbb{N}_0\\ n+r\,\text{odd}}} \cup \left\{\left(\frac{n\pi}{2a}\right)^2 + \frac{\pi^2}{l^2}b_r\left(-\frac{1}{4}\right)\right\}_{\substack{n\in\mathbb{N}\\ r\in\mathbb{N}\\ n+r\,\text{odd}}}, \tag{4.19}$$

and the corresponding normalised eigenfunctions of K are given by the restrictions

$$\psi^{(j)}_{r,n} := \sqrt{2}\,\phi^{(j)}_{r,n} \restriction (0, l) \times (-a, a)$$

where $(r, n) \in \mathbb{N} \times \mathbb{N}$ if $j = 1$ and $(r, n) \in \mathbb{N}_0 \times \mathbb{N}$ if $j = 2$. That the normalisation factor $\sqrt{2}$ is correct follows from the final equations in Remark 4.3 and equations (4.16) and (4.17).

The kind reader surely feels an awkwardness in the last paragraph. Before we proceed any further let us therefore try to simplify our notation by putting

$$\mathbb{N}_1 := \mathbb{N} \times \mathbb{N} \quad \text{and} \quad \mathbb{N}_2 := \mathbb{N}_0 \times \mathbb{N}\,.$$

To show that the right-hand side of (4.19) determines *all* the eigenvalues of K, we need the following result analogous to Proposition (1).

Proposition 3. $\{\psi^{(j)}_{r,n}\}_{j=1,2,\,(r,n)\in\mathbb{N}_j,\,r+n\,\textit{is odd}}$ is a complete orthonormal set in $L^2((0, l) \times (-a, a))$.

Proof. The property that the set $\{\phi^{(j)}_{r,n}\}_{j=1,2,\,(r,n)\in\mathbb{N}_j}$ is a complete orthonormal set in $L^2((-l, l) \times (-a, a))$ is equivalent to the validity of the Parseval equality

$$\|f\|^2 = \sum_{j=1,2,\,(r,n)\in\mathbb{N}_j} |(\phi^{(j)}_{r,n}, f)|^2 \tag{4.20}$$

for every $f \in L^2((-l, l) \times (-a, a))$. Given an arbitrary $g \in L^2((0, l) \times (-a, a))$, we define the extension $f \in L^2((-l, l) \times (-a, a))$ by

$$f(s, t) := \begin{cases} g(s, t) & \text{if} \quad s > 0\,, \\ g(s + l, -t) & \text{if} \quad s < 0\,. \end{cases}$$

By an obvious integral substitution, it is straightforward to check the identity

$$\|f\|^2 = 2\,\|g\|^2\,. \tag{4.21}$$

At the same time, using in addition to the substitution the symmetry property (4.18) we have

$$\begin{aligned}(\phi_{r,n}^{(j)},\, f) &= \int_{(-l,0)\times(-a,a)} \phi_{r,n}^{(j)}(s,t) g(s+l,-t)\,\mathrm{d}s\mathrm{d}t \\ &\quad + \int_{(0,l)\times(-a,a)} \phi_{r,n}^{(j)}(s,t) g(s,t)\,\mathrm{d}s\mathrm{d}t \\ &= \int_{(0,l)\times(-a,a)} \phi_{r,n}^{(j)}(s-l,-t) g(s,t)\,\mathrm{d}s\mathrm{d}t \\ &\quad + \frac{1}{\sqrt{2}} \int_{(0,l)\times(-a,a)} \psi_{r,n}^{(j)}(s,t) g(s,t)\,\mathrm{d}s\mathrm{d}t \\ &= \frac{(-1)^{r+n+1}}{\sqrt{2}} \int_{(0,l)\times(-a,a)} \psi_{r,n}^{(j)}(s,t) g(s,t)\,\mathrm{d}s\mathrm{d}t \\ &\quad + \frac{1}{\sqrt{2}} \int_{(0,l)\times(-a,a)} \psi_{r,n}^{(j)}(s,t) g(s,t)\,\mathrm{d}s\mathrm{d}t \\ &= \frac{1}{\sqrt{2}} \left((-1)^{r+n+1}+1\right) (\psi_{r,n}^{(j)},\, g)\,. \end{aligned} \tag{4.22}$$

Putting (4.21) and (4.22) into (4.20), we get the Parseval inequality

$$\|g\|^2 = \sum_{\substack{j=1,2,\,(r,n)\in\mathbb{N}_j \\ r+n \text{ is odd}}} \left|(\psi_{r,n}^{(j)},\, g)\right|^2,$$

which is equivalent to the desired completeness result. □

Remark 4.4. The smallest eigenvalue of the operator $K = H + V_0$ is given by (indeed, note equations (4.19) and (4.15))

$$\left(\frac{\pi}{2a}\right)^2 + \frac{\pi^2}{l^2} a_0\left(-\frac{1}{4}\right).$$

Therefore, the estimate of Proposition 2 is equivalent to

$$\underbrace{\left(\frac{\pi}{2a}\right)^2}_{\lambda_{0,1}} + \frac{\pi^2}{l^2} a_0\left(-\frac{1}{4}\right) \le \lambda_{0,1} - \frac{14\sqrt{3}-24}{l^2},$$

or (according to Mathematica)

$$-0.3063466 \approx \pi^2 a_0\left(-\frac{1}{4}\right) \le -14\sqrt{3}+24 \approx -0.2487113\,.$$

4.3 Numerical experiments

In this section we briefly present results of our numerical experiments. In order to find a numerical approximation to eigenvalues of operators H and

K we employ the finite difference discretization of the operator in question as discussed in Chapter 3. As already discussed there, the discretization is based on a simple rectangular grid (see Figure 3.1) and the finer the grid is, the better approximation of the original spectrum we expect to get. This effect is demonstrated in Figure 4.4 (fake Möbius) and Figure 4.5 (not-so-fake Möbius). The comparison of the first three eigenvectors of the fake and the not-so-fake Möbius strip can be found on Fig. 4.6. The numerical solution of the full Möbius strip is not presented due to problems with discretization – the normal procedure produces non–symmetrical matrix. This generates difficulties for the algorithm computing the eigenvalues. Further work on the full problem and its numerical implementation is needed.

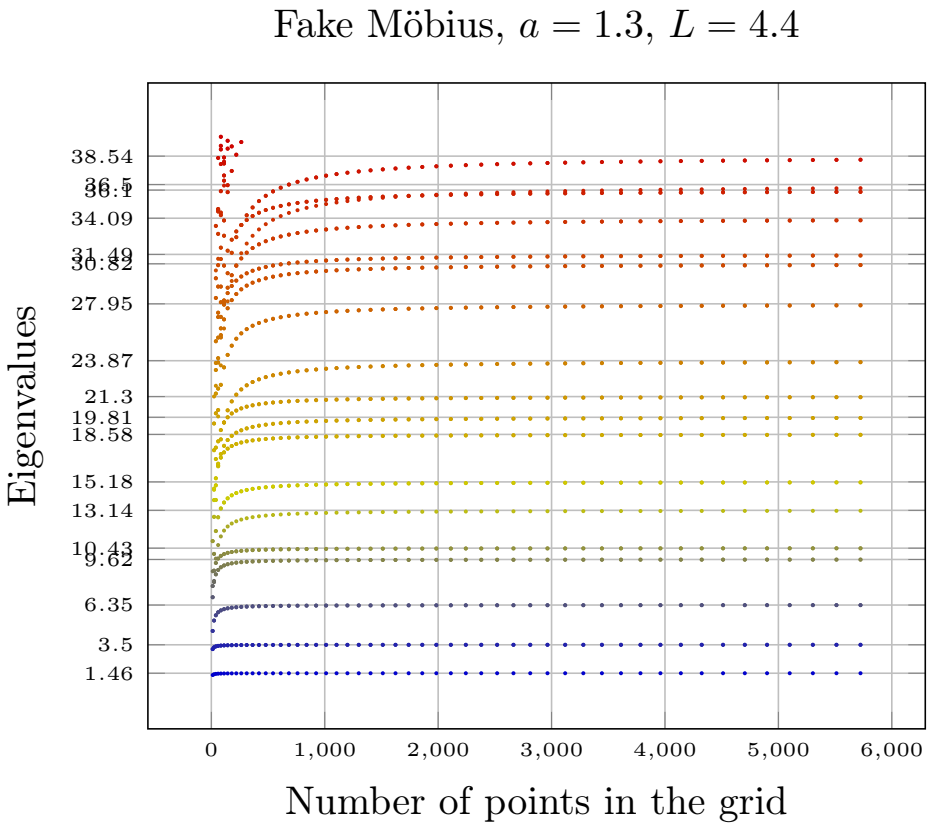

Figure 4.4: Graphical representation of the bottom of $\sigma(H)$ (fake Möbius) and its approximation by the finite difference method. We have chosen $a = 1.3$ and $l = 4.4$. The horizontal axis gives the size of the discretized matrix operator, which is related to the number of points in the grid $(n_t + 1) \cdot (n_s + 1)$ (we have taken $n_t = 2 + i$ and $n_s = 4 + 2i$ with $i = 1, 2, \ldots, 50$). Gray lines indicate the actual eigenvalues of H as given in (4.3)).

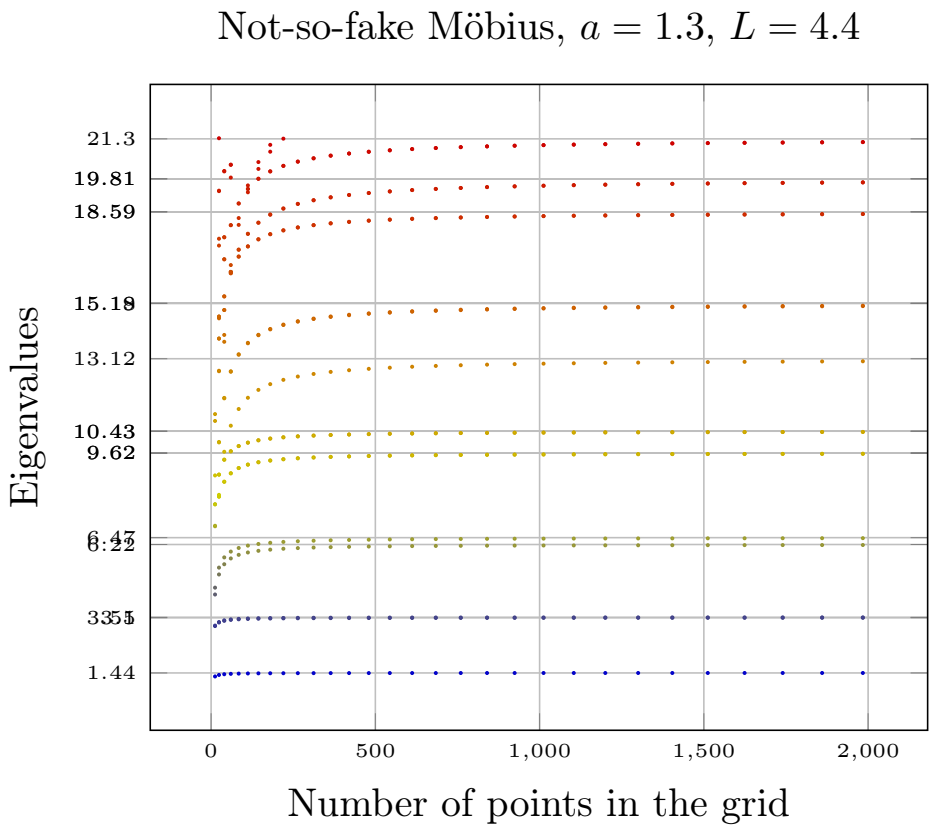

Figure 4.5: Graphical representation of the bottom of $\sigma(K)$ (not-so-fake Möbius) and its approximation by the finite difference method. We have chosen $a = 1.3$ and $l = 4.4$. The horizontal axis gives the size of the discretized matrix operator which is related to the number of points in the grid $(n_t + 1) \cdot (n_s + 1)$ (we have taken $n_t = 2 + i$ and $n_s = 4 + 2i$ with $i = 1, 2, \ldots, 30$). Gray lines indicate the actual eigenvalues of K as given in (4.19)). As one can see on the left hand side of the figure there are few very closely clustered eigenvalues (these are not degeneracies). From the picture it is not obvious that the numerical result captures this effect correctly. Therefore, we present Table 4.1 where one can see the actual numerical values.

i	λ_1	λ_2	λ_3	λ_4	λ_5
1	1.31403	3.1865	3.20382	4.36004	4.61454
2	1.36982	3.31949	3.33614	5.10517	5.35975
3	1.39625	3.38242	3.39876	5.4848	5.73941
4	1.41076	3.41698	3.43316	5.7008	5.95542
5	1.41957	3.43794	3.45403	5.83447	6.0891
6	1.42531	3.45161	3.46763	5.92263	6.17727
7	1.42925	3.46099	3.47698	5.98372	6.23836
8	1.43208	3.46772	3.48367	6.02775	6.28238
9	1.43417	3.47271	3.48864	6.06049	6.31513
10	1.43577	3.4765	3.49241	6.0855	6.34014
11	1.43701	3.47946	3.49536	6.10502	6.35966
12	1.43799	3.48181	3.49769	6.12055	6.37519
13	1.43879	3.4837	3.49958	6.1331	6.38774
14	1.43944	3.48525	3.50112	6.14338	6.39803
15	1.43998	3.48654	3.5024	6.15192	6.40656
16	1.44043	3.48761	3.50347	6.15908	6.41373
17	1.44082	3.48853	3.50438	6.16515	6.41979
18	1.44115	3.4893	3.50516	6.17033	6.42498
19	1.44143	3.48997	3.50583	6.1748	6.42944
20	1.44167	3.49056	3.5064	6.17867	6.43331
21	1.44188	3.49106	3.50691	6.18205	6.43669
22	1.44207	3.49151	3.50735	6.18501	6.43966
23	1.44224	3.4919	3.50774	6.18763	6.44228
24	1.44238	3.49225	3.50809	6.18996	6.4446
25	1.44251	3.49256	3.5084	6.19203	6.44667
26	1.44263	3.49284	3.50868	6.19388	6.44853
27	1.44273	3.49309	3.50892	6.19554	6.45019
28	1.44283	3.49331	3.50915	6.19705	6.45169
29	1.44291	3.49352	3.50935	6.19841	6.45305
30	1.44299	3.4937	3.50953	6.19964	6.45429
∞	1.444177	3.496521	3.512343	6.218488	6.473136

Table 4.1: Five smallest eigenvalues of the operator K (not-so-fake Möbius). We have chosen $a = 1.3$ and $l = 4.4$. The parameter i is related to the grid coarseness, in particular $n_t = 2 + i$ and $n_s = 4 + 2i$. The last row presents the exact value computed by Mathematica (see (4.19)). The values of λ_2 and λ_3 are indistinguishable in Figure 4.5.

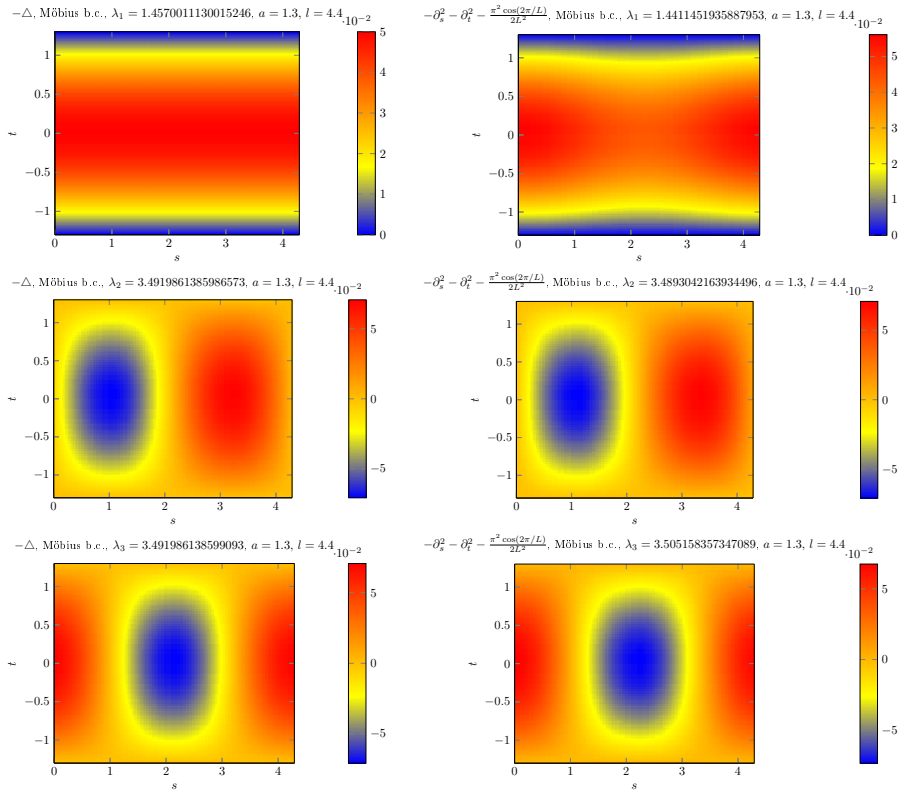

Figure 4.6: Contour plots comparing the first three eigenvectors of the fake Möbius strip (on the left) and of the not-so-fake Möbius strip (on the right). Note that the only visible difference is only for the first eigenvalue.

Conclusions

Our main aim, in this research project, was to correctly define quantum strips in higher dimensions and study the Dirichlet Laplacian on them. Following the process outlined in [9], we deduced the effective potential for narrow strips and compared it with the one already known and studied for ribbons in three dimensions. Secondary aim was to find out the spectrum of the Möbius strip, a special example of a quantum ribbon. Due to the inseparability of its Dirichlet Laplacian, we needed to employ the numerical methods. However, the full model proved to be challenging even for that so two simplified models are presented instead.

In the future, there are two main areas for further investigation. One of them is the proof of the Hardy inequality concerning the twisting term of the effective potential and existence of bound states due to the curvature term. The other is to execute numerical simulations concerning the full Möbius strip and compare it to a cylinder and an annulus.

Bibliography

[1] M. Abramowitz and I. A. Stegun. *Handbook of Mathematical Functions, With Formulas, Graphs, and Mathematical Tables*. Dover Publications, 1974.

[2] R. L. Bishop. There is more than one way to frame a curve. *American Mathematiacal Monthly*, 82:246–251, 1975.

[3] J. Blank, P. Exner, and M. Havlíček. *Lineární operátory v kvantové fyzice*. Karolinum, 1993.

[4] H. Bogunovic, J. M. Pozo, R. Cardenes, M. C. Villa-Uriol, R. Blanc, M. Piotin, and A. F. Frangi. Automated landmarking and geometric characterization of the carotid siphon. *Medical Image Analysis*, 16(4):889–903, 2012.

[5] D. Borisov, P. Exner, R. Gadyl'shin, and D. Krejčiřík. Bound states in weakly deformed strips and layers. *Annales Henri Poincaré*, 2(3):553–572, jun 2001.

[6] C. H. O. Chui and P. A. Pearce. Finitized Conformal Spectra of the Ising Model on the Klein Bottle and Möbius Strip. *Journal of Statistical Physics*, 107(5/6):1167–1205, 2002.

[7] J. Dittrich and J. Kříž. Bound states in straight quantum waveguides with combined boundary conditions. *Journal of Mathematical Physics*, 43:3892–3915, 2002.

[8] *NIST Digital Library of Mathematical Functions*. http://dlmf.nist.gov/, Release 1.0.15 of 2017-06-01. F. W. J. Olver, A. B. Olde Daalhuis, D. W. Lozier, B. I. Schneider, R. F. Boisvert, C. W. Clark, B. R. Miller and B. V. Saunders, eds.

[9] P. Duclos, P. Exner, and D. Krejcirik. Locally curved quantum layers. *Ukrainian J. Phys.*, pages 595–601, 2000.

[10] P. Exner, P. Freitas, and D. Krejciřík. A lower bound to the spectral threshold in curved tubes. *Proceedings of the Royal Society of London Series A*, 460:3457–3467, December 2004.

[11] P. Exner and A. Minakov. Curvature-induced bound states in Robin waveguides and their asymptotical properties. *Journal of Mathematical Physics*, 55(12):122101, December 2014.

[12] P. Exner and P. Seba. Bound states in curved quantum waveguides. *Journal of Mathematical Physics*, 30(11):2574–2580, nov 1989.

[13] R. T. Farouki and S. Q. Li. Optimal tool orientation control for 5-axis CNC milling with ball-end cutters. *Computer Aided Geometric Design*, 30(2):226–239, 2013.

[14] P. W. Fowler and L. W. Jenneskens. Geometric localisation in Möbius π systems. *Chemical Physics Letters*, 427(1-3):221–224, August 2006.

[15] P. Freitas and D. Krejčiřík. Waveguides with Combined Dirichlet and Robin Boundary Conditions. *Mathematical Physics, Analysis and Geometry*, 9(4):335–352, Febuary 2007.

[16] Y. Gaididei, A. Goussev, V. P. Kravchuk, O. V. Pylypovskyi, J. M. Robbins, D. D. Sheka, V. Slastikov, and S. Vasylkevych. Magnetization in narrow ribbons: curvature effects. *ArXiv e-prints*, January 2017.

[17] J. Goldstone and R. L. Jaffe. Bound states in twisting tubes. *Phys. Rev. B*, 45:14100–14107, 1992.

[18] J. Gravesen and M. Willatzen. Eigenstates of möbius nanostructures including curvature effects. *Phys. Rev. A*, 72:032108, Sep 2005.

[19] Z. L. Guo, Z.R. Gong, H. Dong, and C. P. Sun. Möbius graphene strip as a topological insulator. *Physical Review B*, 80(19), nov 2009.

[20] S. Haag, J. Lampart, and S. Teufel. Generalised Quantum Waveguides. *Annales Henri Poincaré*, 16:2535–2568, November 2015.

[21] A. J. Hanson and H. Ma. Parallel transport approach to curve framing. Technical report, Indiana University, Bloomington, IN 47405, January 1995.

[22] W. Klingenberg and D. Hoffman. *A course in differential geometry.* Graduate Texts in Mathematics. Springer, 1978.

[23] M. Kolb and D. Krejčiřík. The Brownian traveller on manifolds. *Journal of Spectral Theory*, August 2011.

[24] R. S. Krausshar. The Helmholtz Operator on Higher Dimensional Möbius Strips Embedded in $\mathbb{R}^4$. *Advances in Applied Clifford Algebras*, 22(3):745–755, September 2012.

[25] R. S. Krausshar. The Klein-Gordon Operator on Möbius Strip Domains and the Klein Bottle in $\mathbb{R}^n$. *Mathematical Physics, Analysis and Geometry*, 16(4):363–379, December 2013.

[26] D. Krejcirik. Hardy inequalities in strips on ruled surfaces. *Journal of Inequalities and Applications*, November 2005.

[27] D. Krejčiřík. Quantum strips on surfaces. *Journal of Geometry and Physics*, 45:203–217, February 2003.

[28] D. Krejčiřík and H. Šediváková. The Effective Hamiltonian in Curved Quantum Waveguides Under Mild Regularity Assumptions. *Reviews in Mathematical Physics*, 24:1250018, August 2012.

[29] W. Kuhnel. *Differential geometry: curves - surfaces - manifolds*. American Mathematical Society, 2 edition, 2005.

[30] P. Li and Z. Zhang. Continuous-time quantum walks on nonorientable surfaces: analytical solutions for Möbius strips and Klein bottles. *Journal of Physics A: Mathematical and Theoretical*, 45(28):285301, June 2012.

[31] M. Lundgren, A. J. Niemi, and F. Sha. Protein loops, solitons, and side-chain visualization with applications to the left-handed helix region. *Physical Review E*, 85(6):13, 2012.

[32] S. A. Nazarov and M. Specovius-Neugebauer. Selfadjoint Extensions of the Neumann Laplacian in Domains with Cylindrical Outlets. *Communications in Mathematical Physics*, 185(3):689–707, May 1997.

[33] A. J. Niemi. Gauge fields, strings, solitons, anomalies, and the speed of life. *Theoretical and Mathematical Physics*, 181(1):1235–1262, 2014.

[34] R. Novák. Bound states in waveguides with complex Robin boundary conditions. *Asymptotic Analysis*, 96(3-4):251–281, Feb 2016.

[35] B. O'Neill. *Elementary differential geometry*. Academic Press, 1966.

[36] M. Reed and B. Simon. *Methods of modern mathematical physics. Analysis of operators*, volume 4 of *Methods of Modern Mathematical Physics*. Academic Press, 1978.

[37] E. L. Starostin and G. H. M. van der Heijden. Equilibrium Shapes with Stress Localisation for Inextensible Elastic Möbius and Other Strips. *Journal of Elasticity*, 119(1-2):67–112, August 2014.

[38] J. Tolar. *On a quantum mechanical d'Alembert principle*, pages 268–274. Springer Berlin Heidelberg, Berlin, Heidelberg, 1988.

[39] K. Yakubo, Y. Avishai, and D. Cohen. Persistent currents in Möbius strips. *Physical Review B*, 67(12), mar 2003.

[40] K. Zahradová. Frame defined by parallel transport for curves in any dimension, 2016.